ISSN 2616-5880 Vol. 7, Issue 1: 108-114, DOI: 10.25236/AJMC.2026.070115

Influence of mullite whisker incorporation on the surface morphology of PZT ceramic

Geng Hou[1,2,a], Zhenzhong Sun[1,b,*], Yang Yang[1]

[1]*School of Mechanical Engineering, Dongguan University of Technology, Dongguan, 523808, China*
[2]*School of Materials Science and Engineering, Xi'an Jiaotong University, Xi'an, 710049, China*
[a] *geng.hou@qq.com,* [b]*sunzz@dgut.edu.cn*
**Corresponding author*

Abstract: *This study attempted to incorporate mullite whiskers into lead zirconate titanate (PZT) piezoelectric ceramics, and a PZT-based composite ceramic containing 1 wt% and 2 wt% whiskers was fabricated. During the characterization of the microstructure of the samples using scanning electron microscopy, it was unexpectedly observed that the introduction of the whiskers led to the formation of distinct pit-like defects on the surface of the PZT ceramic, with whisker enrichment occurring in regions adjacent to the pits. Based on an analysis of the thermophysical properties of the constituent materials, a possible formation mechanism for the pits is proposed: during the cooling stage of sintering, the mullite whiskers, which possess a higher coefficient of thermal expansion than the PZT matrix, undergo larger contraction. Through interfacial bonding, the whiskers exert a dragging effect on the surrounding PZT matrix, driving the matrix to migrate toward the whisker-enriched regions. This migration results in a volume void in the whisker-depleted regions, ultimately leading to the formation of surface pits. In addition, the influence of whisker content on the degree of pit defects was also briefly analyzed.*

Keywords: *Mullite whisker; PZT ceramic; Surface morphology; Pit*

1. Introduction

Lead zirconate titanate (PZT) piezoelectric ceramics exhibit excellent piezoelectric properties [1,2] and have become widely used and commercially available piezoelectric ceramics [3,4]. However, their inherent brittleness and less-than-ideal mechanical properties limit their application in certain contexts [5,6]. The introduction of whiskers is considered an effective approach to improving the mechanical properties of brittle ceramics [5-7]. Mullite whiskers, known for their high strength, high-temperature resistance, and good thermal stability, have been demonstrated to enhance the mechanical properties of oxide ceramics [8,9]. Nevertheless, studies on incorporating mullite whiskers into PZT ceramics remain limited.

In this work, a PZT ceramic containing mullite whiskers were prepared, and distinct whisker-like structures along with whisker-related composition were observed in the sintered ceramics. Meanwhile, a comparative observation revealed the presence of noticeable pit-like micro-structures on the surface of the whisker-containing samples. Based on scanning electron microscopy microstructural observations and an analysis of the constituent material properties, this study attempts to explain the formation mechanism of these pits, with the aim of providing a reference for microstructural optimization of PZT-based whisker-reinforced composite ceramics.

2. Materials and Preparation Methods

2.1. Material Composition

The composition of the PZT-based ceramic powder used in the experiments is shown in Table 1. During the powder mixing process, specific proportions of dispersant, binder, and defoamer were added to obtain the PZT-based ceramic powder intended for subsequent mixing with mullite whiskers. On this basis, the newly obtained PZT-based ceramic powder was mixed with mullite whiskers at a specific weight ratio to produce the green body material for forming and sintering. In this work, two formulations were prepared, containing 0 wt%, 1 wt% and 2 wt% whisker content by mass, respectively. The mullite whiskers had a diameter of 0.5-1.0 μm and a length of 15-20 μm. The microstructure of the mixed powder of mullite whiskers and PZT ceramic is provided in the Appendix.

ISSN 2616-5880 Vol. 7, Issue 1: 108-114, DOI: 10.25236/AJMC.2026.070115

Table 1: Composition of the PZT ceramic powder mixture.

Composition	Pb_3O_4	ZrO_2	TiO_2	$MnCO_3$	$Ca_2Fe_2O_5$
Content (% wt)	65.5	19.8	11.9	2.28	0.50

2.2. Preparation Process

As shown in Figure 1, the preparation process for the PZT ceramic with mullite whiskers consists of the following nine steps:

Step 1 – Mixing of ceramic powders: Lead tetroxide (Pb_3O_4), zirconium oxide (ZrO_2), titanium dioxide (TiO_2), manganese carbonate ($MnCO_3$), and dicalcium ferrite ($Ca_2Fe_2O_5$) powders are placed in a stirred ball mill, and water equal in weight to the powder mixture is added. The mixture is then milled for 8 hours.

Step 2 – Drying: The mixed raw materials are placed in an air atmosphere at 120 °C in a high-temperature chamber for 2 days.

Step 3 – Presintering: The dried raw material blocks are presintered in a muffle furnace at 850 °C for 9 hours.

Step 4 – Crushing: The presintered blocks are crushed using a crusher.

Step 5 – Powder grinding: The crushed powder is further ground using a stirred ball mill followed by a circulating sand mill. During this process, water equal in weight to the powder was added, together with a dispersant, a binder, and a defoamer, following the proportions of 10 mL of water-based defoamer, 10 mL of CERAMO D-134C cationic water-soluble polymer dispersant, and 11 mL of CERAMO PB-72 acrylate-based binder per kilogram of powder.

Step 6 – Drying into powder: The powder slurry is dried using a centrifugal spray dryer.

Step 7 – Whisker incorporation: Based on the proportions given in Table 1, 1 wt% or 2 wt% mullite whiskers are added to the PZT ceramic matrix powder, and the mixture is homogenized by oscillation.

Step 8 – Compaction: Using a mold, 6 g of the mixed powder containing whiskers is pressed into cylindrical thin-disc green compacts with a diameter of 20 mm. The compaction pressure is 300 MPa.

Step 9 – Sintering: The green compacts are pressurelessly sintered in a muffle furnace under an air atmosphere at 1200 °C for 2 hours.

Figure 1: Schematic diagram of the preparation process of PZT ceramic incorporating mullite whiskers.

ISSN 2616-5880 Vol. 7, Issue 1: 108-114, DOI: 10.25236/AJMC.2026.070115

3. Results and Discussions

3.1. Morphological Comparison

From Figures 2 and 3, it can be observed that the surface of the material without whiskers appears obviously smoother than that of the whisker-containing material, where distinct pit-like defects are present. As shown in Figure 3(b), taking the material with 1 wt% whiskers as an example (the pit microstructure of the 2 wt% whisker-containing material is similar), apparent signs of whisker enrichment are observable in some regions adjacent to the pits, which is also consistent with the energy-dispersive spectroscopy (EDS) result for aluminum (mullite whisker is composed primarily of alumina [10]). Furthermore, the distribution of the whiskers is not entirely uniform; rather, some regions exhibit a higher concentration of whiskers while others show fewer, indicating a certain degree of agglomeration. In addition, the distinct whisker structures and chemical compositions presented in Figure 3(b) also indicate that the PZT components did not show obvious signs of chemical erosion on the mullite whiskers during the sintering process.

Figure 2: Macroscopic morphologies of sintered ceramic samples.

3.2. Morphological Comparison

Before reaching the sintering temperature, Pb_3O_4 in the PZT powder decomposes at around 530~547°C into PbO and oxygen [11]. Since the melting point of PbO is only 830~897°C [11], a liquid phase is present during sintering, which facilitates the rearrangement of the microstructure and reduces the interparticle forces. As shown in Figure 4, for the PZT ceramics containing mullite whiskers, the axial coefficient of thermal expansion (CTE) of mullite whiskers is approximately 4.7×10^{-6}/K [12-14], whereas the CTE of the isotropic PZT ceramic matrix ranges from 0.5 to 3.6×10^{-6}/K [15]. Given that the CTE of the whiskers is higher than that of the pure PZT matrix, during the cooling stage of the sintered sample from the molten state, the contraction of the whiskers is considerably larger than that of the surrounding matrix. Owing to the non-uniform distribution of whiskers, when multiple whisker-enriched regions are spatially adjacent to each other, they exert dragging effects on the matrix in the intervening whisker-depleted zone from different directions. This multidirectional dragging and pulling causes the PZT matrix in the depleted region to migrate towards the surrounding enriched regions, eventually leading to the formation of a depression pit at the original site, which results from local loss of the matrix material.

3.3. Effect of whisker content on pit defects

To accurately and objectively quantify the area fraction of pit defects on the material surface, the open-access scientific image analysis software ImageJ was employed [16]. As shown in Table 2, the colour macroscopic images were first converted into 8-bit grayscale images using ImageJ. Owing to variations in the original colours among different samples, the degree of colour contrast between defect-free regions and pit defects differed from sample to sample. To minimise this variation and allow an objective comparison of pit area fractions under identical quantitative conditions, background correction was performed using the rolling-ball algorithm (Subtract Background) in ImageJ. To maintain consistency with the software's default settings and ensure the reproducibility of the processing procedure, the rolling-ball radius was set to the default value of 50 pixels for all images. This pixel value is larger than the radius of the largest pores present in any image, which facilitates accurate background estimation. Finally, the grayscale threshold was adjusted via the Threshold option in ImageJ so that the red regions (as indicated in step 2 of Table 2) covered all visible pore areas. Furthermore, for objective

ISSN 2616-5880 Vol. 7, Issue 1: 108-114, DOI: 10.25236/AJMC.2026.070115

analysis and comparison, the same grayscale threshold of 140 was applied to all images when evaluating the extent of pit defects.

The area fractions of pit defects on the material surface for samples without and with whiskers are presented in Figure 5. It can be observed from the figure that as the whisker content rises from 1 wt% to 2 wt%, the pit area fraction initially increases. This may be attributed to whisker agglomeration in a greater number of regions. Therefore, suppressing whisker agglomeration could be one of the key factors for improving the surface quality of whisker-containing PZT ceramics during the fabrication process.

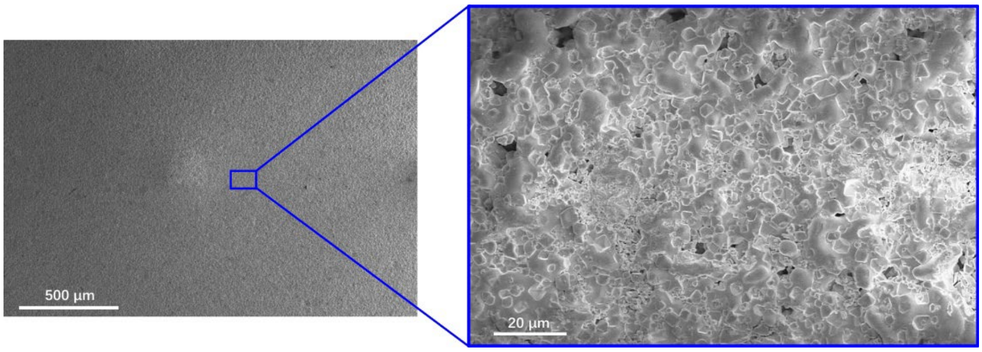

(a) Whisker-free

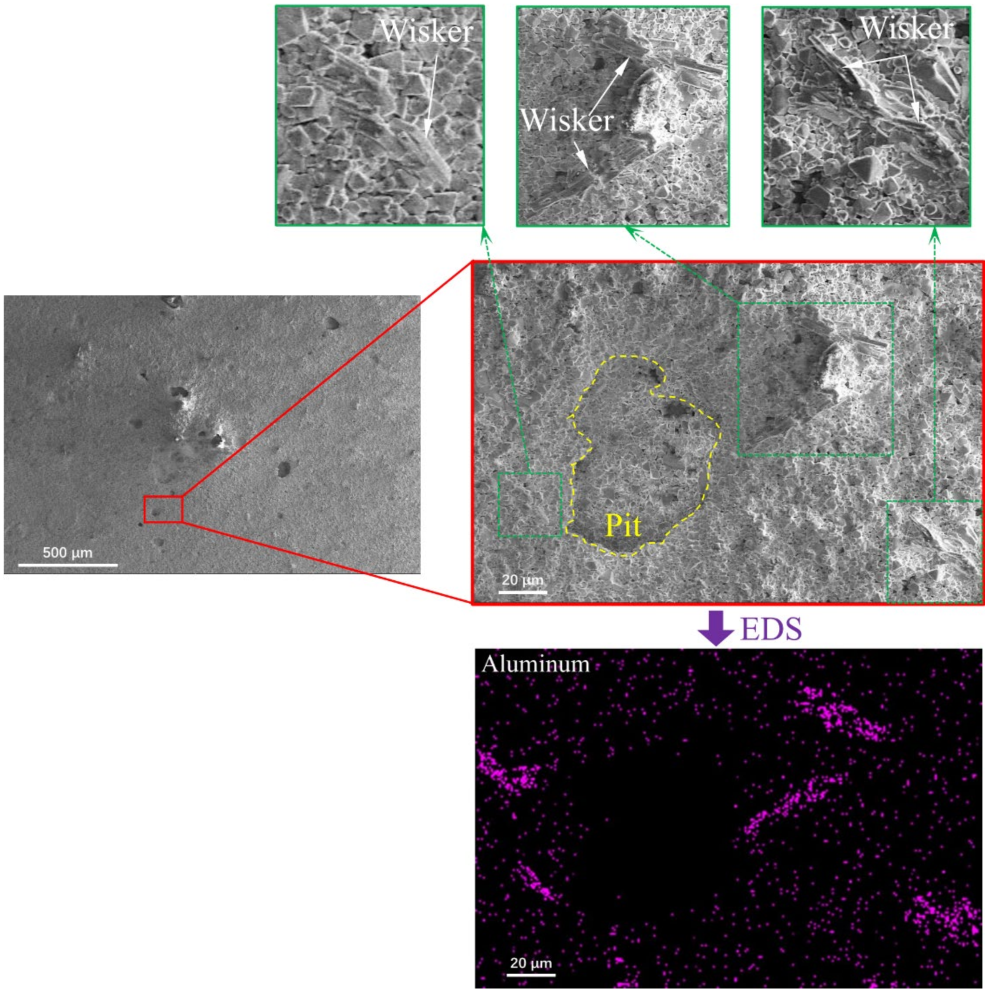

(b) 1 wt% whisker-containing

Figure 3: Microstructure observed using scanning electron microscopy.

Note: Mullite whiskers are composed primarily of alumina [10], whereas PZT ceramic contains no aluminum; thus, the distribution of whiskers is identified via aluminum elemental spectroscopy.

ISSN 2616-5880 Vol. 7, Issue 1: 108-114, DOI: 10.25236/AJMC.2026.070115

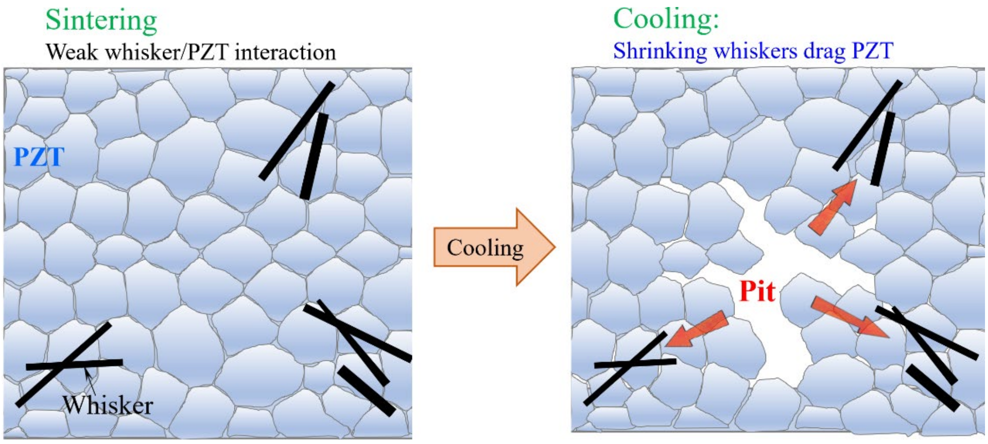

Figure 4: Schematic diagram of the pit formation mechanism in mullite whisker-containing PZT ceramics.

Table 2: Procedure for calculating the pit area fraction on material surfaces using software ImageJ.

Process	Whisker-free	1 wt% whisker-containing	2 wt% whisker-containing
Step 0: Untreated image	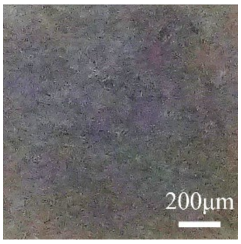	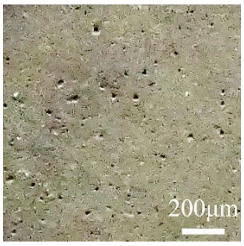	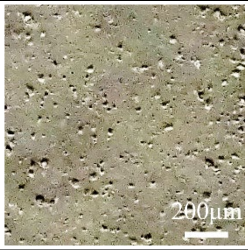
Step 1: Converted to 8-bit grayscale image	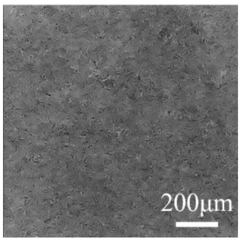	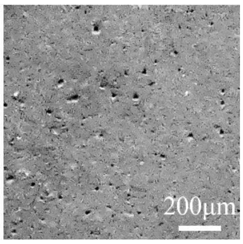	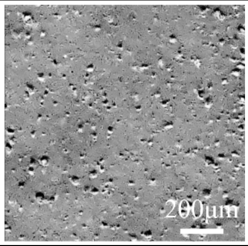
Step 2: Background correction	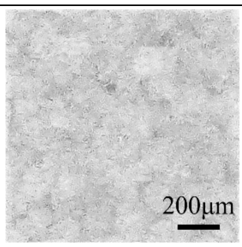	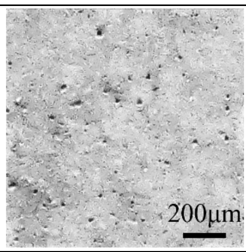	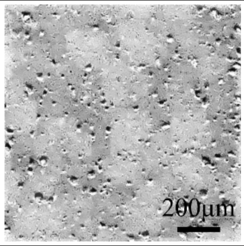
Step 3: Adjust the grayscale threshold (red indicates pit regions with high gray levels)	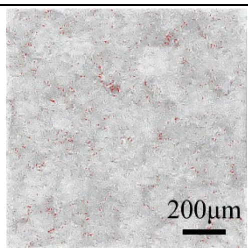	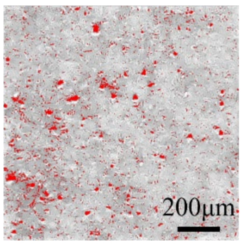	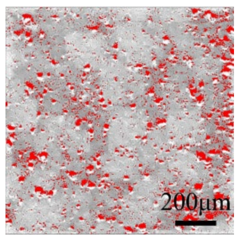
Result	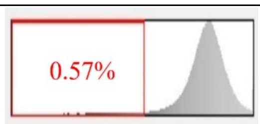	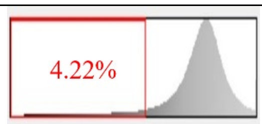	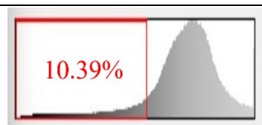

ISSN 2616-5880 Vol. 7, Issue 1: 108-114, DOI: 10.25236/AJMC.2026.070115

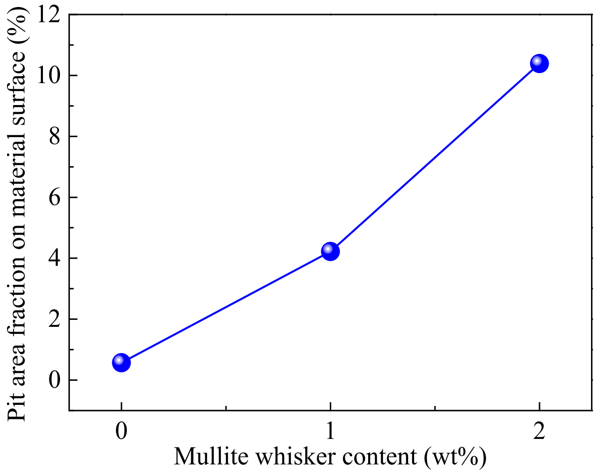

Figure 5: Relationship between mullite whisker content and the pit area fraction on material surface.

4. Conclusions

In this study, PZT ceramics containing mullite whiskers were prepared. On this basis, the formation mechanism of pit-like surface defects in the composite ceramics induced by the introduction of whiskers was analyzed, leading to the following conclusions.

(1) PZT ceramics containing mullite whiskers can be prepared by introducing mullite whiskers into the PZT matrix followed by pressureless sintering in a high-temperature air atmosphere. Distinct whisker structures and compositions can be detected in the as-obtained material, without obvious evidence of chemical erosion.

(2) Compared with whisker-free PZT ceramics, PZT ceramics containing mullite whiskers exhibit distinct pit defects on the surface, and the area fraction of pits tends to increase as the whisker content rises from 1 wt% to 2 wt%. The formation of these pits may be mainly attributed to the difference in thermal expansion coefficient between the mullite whiskers and the PZT matrix. During the cooling process, the dragging effect of the whiskers on the PZT matrix induces the migration of matrix material toward whisker-enriched regions, thereby leading to pit formation in whisker-depleted regions.

(3) Based on the experimental and analytical results of this work, attention should be paid to the uniformity of whisker distribution and the surface defects induced by thermal expansion mismatch during the fabrication of PZT-based whisker-reinforced composite ceramics, in order to optimize the microstructure and suppress the formation of defects.

Appendix

The microstructures of the mullite whiskers and the PZT powder mixture, as observed by scanning electron microscopy, are shown in Figures A1.

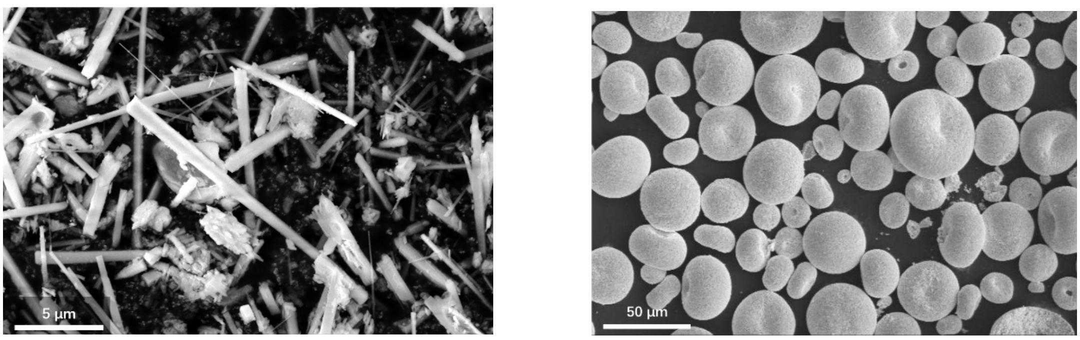

(a) Mullite whisker (b) PZT powder mixture

Figure A1: Microscopic morphology of the Mullite whiskers and PZT powder mixture.

ISSN 2616-5880 Vol. 7, Issue 1: 108-114, DOI: 10.25236/AJMC.2026.070115

Acknowledgements

This investigation was supported by Startup Foundation for Postdoctoral Talent of Dongguan University of Technology (No. 221110348006).

References

[1] AK Zak, ShT Yazdi, ME Abrishami, AM Hashim. A review on piezoelectric ceramics and nanostructures: fundamentals and fabrications [J]. Journal of the Australian Ceramic Society, 2024, 60: 723-753.
[2] DM Pan. Lead zirconate titanate (PZT) piezoelectric ceramics: applications and prospects in human motion monitoring [J]. Ceramics-Silikáty, 2024, 68(3): 444-458.
[3] KS Arya, RP Singh, T Chakrabarti. Novel liquid–phase flash sintering of lead zirconate titanate piezo-ceramics [J]. Journal of the American Ceramic Society, 2024, 107: 8007-8022.
[4] SR Sangawar, B Praveenkumar. Structural and electrical properties of low temperature sintered PZT ceramics [J]. Ferroelectrics, 2017, 517: 66-74.
[5] HB Li, Y Li, DW Wang, R Lu, J Yuan, MS Cao. Effects of ZnO nanoneedles addition on the mechanical and piezoelectric properties of hard PZT-based composites [J]. Journal of Materials Science: Materials in Electronics, 2013, 24: 1463-1468.
[6] T Yamamoto, H Igarashi, K Okazaki. Electrical and mechanical properties of SiC whisker reinforced PZT ceramics [J]. Ferroelectrics, 1985, 63: 281-288.
[7] PF Becher, C-H Hsueh, P Angelini, TN Tiegs. Toughening behavior in whisker-reinforced ceramic matrix composites [J]. Journal of the American Ceramic Society, 1988, 71(12): 1050-1061.
[8] JH Zhang, HD Wu, SX Zhang, JS Yu, SE Hou. Preparation of mullite whiskers and their enhancement effect on ceramic matrix composites [J]. Journal of Wuhan University of Technology-Materials Science Edition, 2013, 28: 471-475.
[9] T Robertson. Mullite whisker enhanced zirconia toughened alumina ceramic matrix composite for high temperature applications [D]. Ottawa, Ontario: Carleton University, 2014.
[10] H Schneider, RX Fischer, J Schreuer. Mullite: crystal structure and related properties [J]. Journal of the American Ceramic Society, 2015, 98(10): 2948-2967
[11] D Risold, J-I Nagata, RO Suzuki. Thermodynamic description of the Pb-O system [J]. Journal of Phase Equilibria, 1998, 19(3): 213-233.
[12] WM Kriven, JW Palko, S Sinogeikin, JD Bass, A Sayir, G Brunauer, H Boysen, F Frey, J Schneider. High temperature single crystal properties of mullite [J]. Journal of the European Ceramic Society, 1999, 19: 2529-2541.
[13] J-S Park, J-H Kim. Coefficients of thermal expansion for single crystal piezoelectric fiber composites [J]. Composites: Part B, 2007, 38: 795-799.
[14] H Hoshyarmanesh, N Ebrahimi, A Jafari, P Hoshyarmanesh, M Kim, H-H Park. PZT/PZT and PZT/BiT composite piezo-sensors in aerospace SHM applications: photochemical metal organic + infiltration deposition and characterization [J]. Sensors, 2019, 19(1): 13.
[15] CTS Denmark A/S (formerly Ferroperm Piezoceramics). What is the thermal expansion coefficient for Ferroperm PZT? [EB/OL]. [2026-06-06]. https://www.ferropermpiezoceramics.com/wp-content/uploads/2019/03/TEC.pdf.
[16] AB Schroeder, ETA Dobson, CT Rueden, P Tomancak, F Jug, KW Eliceiri. The ImageJ ecosystem: Open-source software for image visualization, processing, and analysis [J]. Protein Science, 2021, 30(1): 234-249.